Parametric Weight Evaluation of Joined Wings by Structural Optimization

Hirokazu Miura* and Albert T. Shyu†
NASA Ames Research Center, Moffett Field, California
and
Julian Wolkovitch‡
ACA Industries, Inc., Torrance, California

Joined-wing aircraft employ tandem wings having positive and negative sweep and dihedral, arranged to form diamond shapes in both plan and front views. An optimization method was applied to study the effects of joined-wing geometry parameters on structural weight. The lightest wings were obtained by increasing dihedral and taper ratio, decreasing sweep and span, increasing fraction of airfoil chord occupied by structural box, and locating the joint inboard of the front wing tip.

Nomenclature

b (or b_F)	= front wingspan
B ($=b_R/b_F$)	= joint location parameter, span ratio
S (S_F+S_R)	= total projected wing area
S_R/S_F	= area ratio (rear wing area/front wing area)
λ_F	= front wing taper ratio
λ_R	= rear wing taper ratio
Λ_F	= front wing quarter-chord sweep angle
Λ_R	= rear wing quarter-chord sweep angle
Γ_F	= front wing dihedral angle
Γ_R	= rear wing dihedral angle
f	= structural box chord/airfoil chord
$t_{\min}$	= minimum material gauge thickness
t/c	= airfoil thickness-to-chord ratio

I. Introduction

JOINED-WING configurations employ tandem lifting surfaces that are arranged to form diamond shapes in both plan view and front view (Fig. 1). Such configurations are expected to have various potential advantages when applied to aircraft and missiles[1] including structural weight reduction, low induced drag, good transonic area distribution, high trimmed maximum lift coefficient, reduced wetted area and parasite drag, direct lift-control capability, direct sideforce-control capability, and good stability and control characteristics. Of these desirable characteristics, the structural weight advantage is one of the critical issues that needs quantitative evaluation. Past studies[2-4] are all preliminary in nature, but they have indicated appreciable weight advantages over the conventional cantilever wing and horizontal tail arrangement. However, these studies focused primarily on a particular configuration and on limited perturbations of the base configuration. Since joined-wing concepts cover wide variations of lifting-surface arrangements and have more complex internal force distributions than those of cantilever wings, it is expected that the structural weight advantages will not be fully exploited unless weight evaluations are carried out over a wide variety of configurations.

The purpose of this paper is to present the trends of the structural weight of the joined wings for the conceptual/preliminary design of medium-sized transport aircraft. To calibrate our procedures, we also carried out several weight estimation studies for cantilever configurations using similar structural models, as shown in the Appendix. However, evaluation of weight advantages or disadvantages of joined-wing configurations compared to cantilever-wing configurations is not the subject of the present paper. Limited trade-off studies of joined wings vs aerodynamically equivalent cantilever wings are found in Refs. 1 and 5.

The topological and geometrical design of the wing impacts the overall aircraft performance and cannot be determined simply by the structural weight advantages. Weight evaluation is one of the disciplines that contributes to the aircraft system synthesis, and, in this context, it is desirable to have an aircraft synthesis program capable of handling joined-wing configurations, including reasonable weight estimation capabilities. Presently, such design tools are not available. Weight estimation schemes used in most of the aerospace industry are based primarily on statistical data of past designs; hence, they are not applicable to joined wings, for which past weight data do not exist. This is the justification for the parametric study reported in the present study. A structural weight minimization capability for arbitrary wing configurations based on the PROSSS system[6] was used in this study. The weight minimization capability is an essential ingredient of this program, due to the necessity of obtaining the best material distribution for each configuration so that fair assessments can be made. Aircraft wing weight involves more than the weight of the main structural box, but the accurate estimation of nonstructural weight distribution is beyond the scope of this study. Recalling that our goal is to provide correct trends instead of the absolute weight of the wing, we defined a consistent but simple procedure to estimate the wing structural weight for various possible configurations. Finite-element models used in this study may not reflect all details of conventional structural

Presented as Paper 85-0642-CP at the AIAA/ASME/ASCE/AHS 26th Structures, Structural Dynamics and Materials Conference, Orlando, FL, April 15-17, 1985; received May 3, 1985; revision received May 29, 1987.

*Aerospace Engineer. Associate Fellow AIAA.
†Research Associate. Currently at FMC Corp., San Jose, California.
‡President. Senior Member AIAA.

modeling techniques, but they are sufficient to capture the weight trends based solely on strength requirements. Structural analysis models, loading conditions, design variable assignments, and constraints were selected to be as consistent as possible throughout the geometry changes. Some nonstructural weights were estimated by means of simple methods described in Sec. IV.

Structural weight minimization was carried out at or near the values of parameters proposed by aircraft design specialists at NASA Ames and at ACA Industries. Over 50 cases have been studied. This set of results did not include all possible configurations, but the results obtained do provide useful information in evaluating many joined-wing designs.

II. Structural Characteristics of Joined Wings

Consider the basic structural arrangement as an idealized diamond-shaped space frame ACBD, as shown in Fig. 1. If the viewpoint is placed in the undeformed plane ADB, the resultant lift force L acting on the left front wing AD and the left rear wing DB can be decomposed into components normal and parallel to this plane, as shown in Fig. 2. The out-of-plane component L_o is resisted by the bending stiffness of the beams AD and BD. The in-plane component L_i contributes to axial tensile forces in AD and to axial compression forces in BD. Since all of the structural material is uniformly loaded to support axial forces, transforming a part of the lift into axial internal forces permits more efficient use of structural material, compared to the cantilever configurations. Now consider the cross section of the wing box as shown in Fig. 3. Although the principal axes of this cross section are not parallel and normal to the out-of-plane bending moment, it is intuitively conjectured that the wing structural material should be located at the largest possible distance away from the hypothetical bending axis x'. This thought led the inventor of the joined-wing concept to the "tilted-beam" concept, which predicted that appreciable structural weight savings might be achieved by concentrating the structural material in the upper leading-edge and lower trailing-edge corners of the structural box, as shown in Fig. 3.[1,5] This concept is intuitively useful in understanding the structural advantages of the joined wings, but the fully stressed design presented in Refs. 2 and 3 indicated that the tilted-beam concept did not predict the minimum weight arrangement for the outboard portions of the wings.

To understand this result, internal force distributions (e.g., bending moments and axial forces) for the joined-wing configuration of Refs. 2 and 3 were calculated (Fig. 4) based on the membrane stress data obtained by finite element analyses. An important observation is that the flatwise bending moment M_x changes sign at about the midspan for both the front and rear wings. Since the chordwise bending moment M_z is always negative (trying to bend the left wing forward), it can be easily understood that the material distribution shown in Fig. 3 may be justified in the region where M_x is negative, i.e., for the inboard section. On the other hand, in the outboard section where M_x is positive, it is better to have the structural material distributed opposite to the pattern shown in Fig. 3, i.e. more materials in the lower leading-edge and upper trailing-edge corners. This observation explains the optimum thickness distributions presented in Refs. 2 and 3.

Although relatively complex internal forces are found in the outboard section, the inboard portion is primarily subjected to the moment pattern predicted by the tilted-beam concept. Since this is the more massive and important load-carrying portion of the wing, the tilted-beam concept is of importance in understanding the optimum structural design of joined wings. The evaluation of the net-weight saving or penalty requires detailed design optimization. It is also necessary to consider the effects of the joined-wing system on the weight of the vertical stabilizer and fuselage, but this is beyond the scope of the present study.

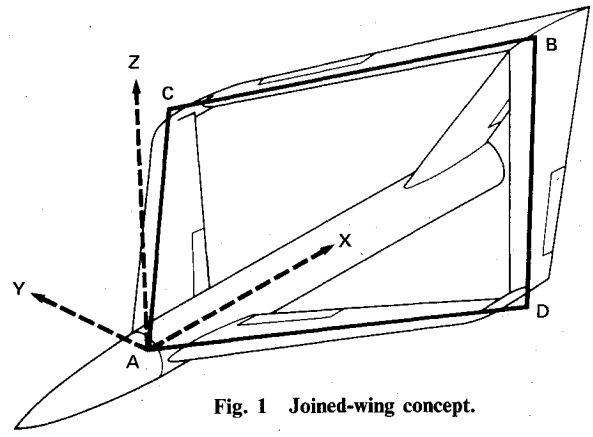

Fig. 1 Joined-wing concept.

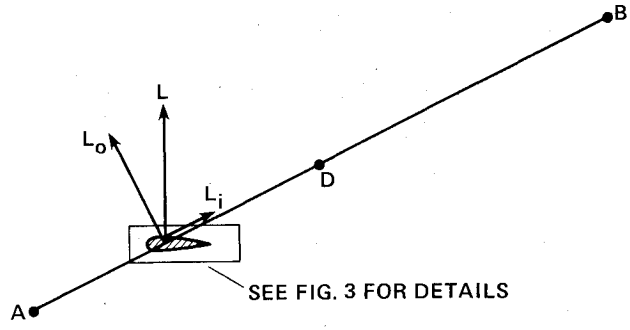

Fig. 2 Lift force decomposition.

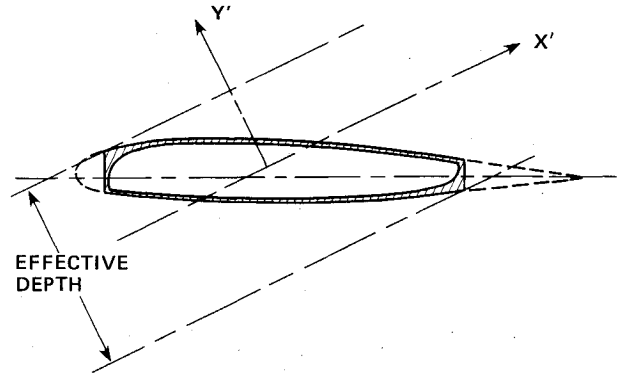

Fig. 3 Wing structure box for joined wing.

III. Structural Design Conditions

Following the standard design method for transport airplane wings, a two-spar wing-box configuration was selected as the primary load-carrying structure. Structural member sizes (in our case, thickness of the cover panels and thickness of ribs and spars) were adjusted to achieve minimum structural weight while supporting prescribed aerodynamic loads without exceeding the allowable stress at any of the points where stress data were computed. A finite-element structural analysis model was constructed for each configuration (Fig. 5). The number of finite elements totals approximately 400 to 450, and these are divided into 55 to 65 groups, so that all elements belonging to the same group have the same thickness. This scheme is known as "design variable linking." Figure 6 presents a typical linking scheme used for both upper and lower skin panel elements in the present study.

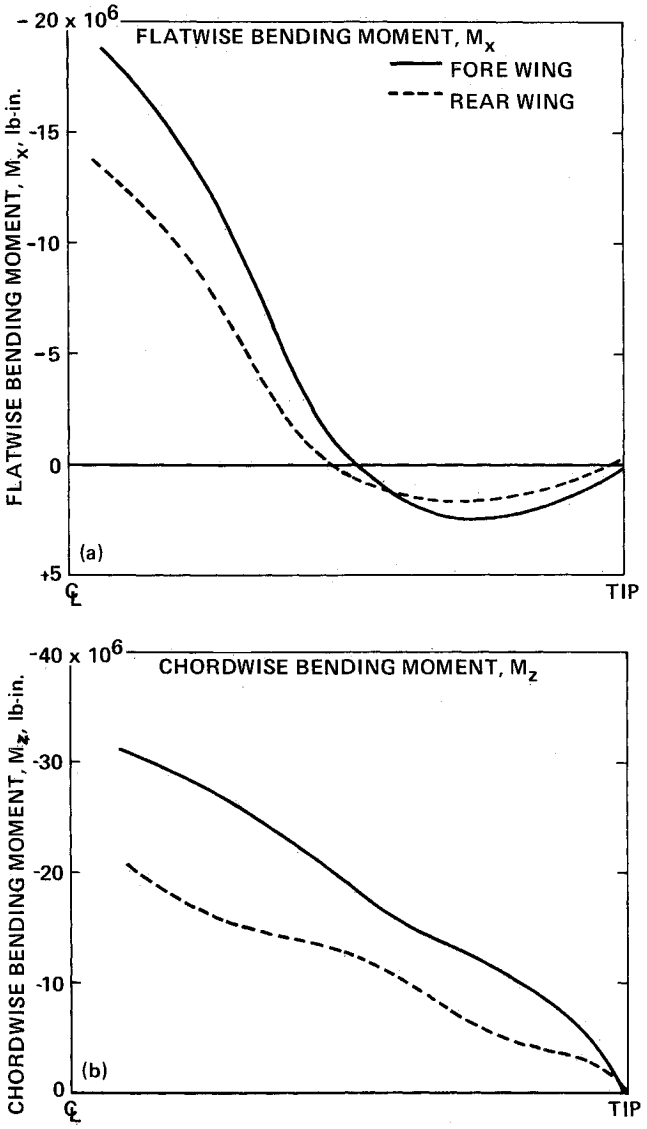

Fig. 4 Flatwise bending moment M_x and chordwise bending movement M_z in front left wings.

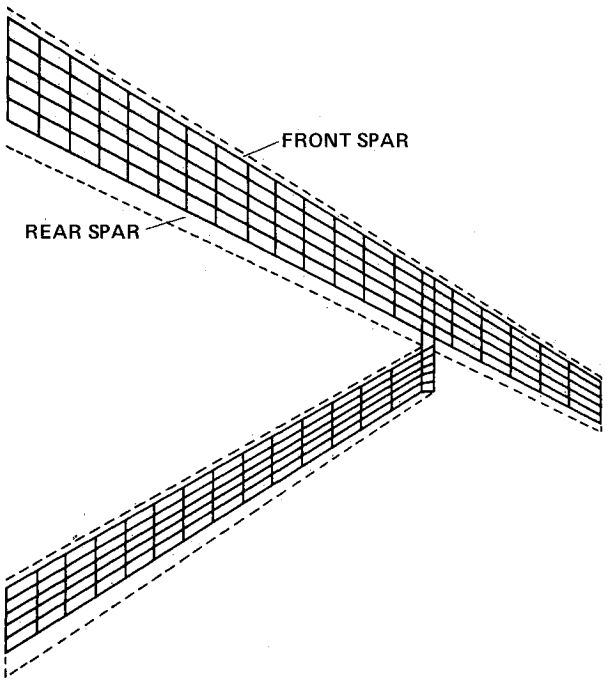

Fig. 5 Example of finite-element model (joint location at 70% of span).

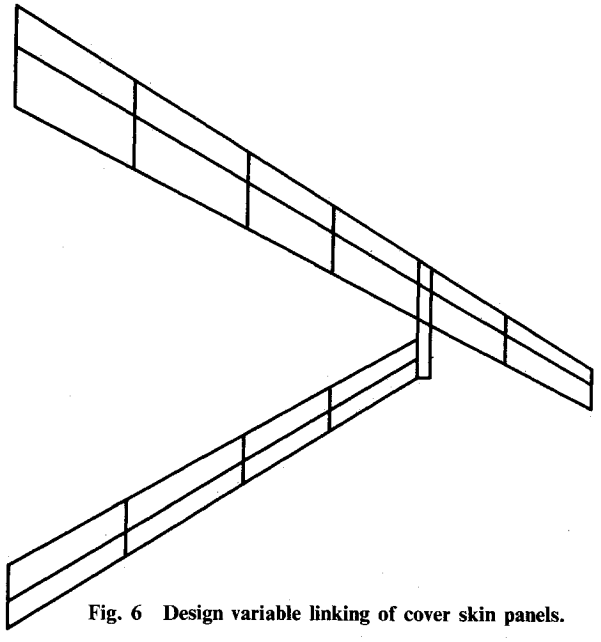

Fig. 6 Design variable linking of cover skin panels.

The structural material considered is limited to an aluminum alloy with an allowable stress limit of 28,000 psi imposed on von Mises combined stress. The material constants are 10.6×10^6 psi for the modulus of elasticity, 0.33 for Poisson's ratio, and 0.1 lb/in.^{3} for specific weight.

Four load conditions are considered, but two of them (negative and positive unit g cases) were identified to be noncritical and deleted from the optimization process. Flight conditions corresponding to the remaining load conditions are 2.5-g maneuver, low $C_L(=0.2)$, forward c.g., and 2.5-g maneuver, high $C_L(=1.0)$, aft c.g. The gross weight of this hypothetical aircraft is assumed to be 170,000 lb. A maneuver load factor of 2.5g and a factor of 1.5 for the ratio between design and ultimate loads yield the ultimate load supported by the wings to be 637,000 lb (see the Appendix for further details). An aerodynamic analysis program that calculates the effects of the downwash of the front wing on the rear wing lift,[7] was used to obtain the distribution of the load between the front and rear wings. Elliptic spanwise load distributions were assumed and two-dimensional airfoil data for NACA 23015 were used to obtain chordwise pressure distributions. The pressure load is applied to the finite-element grid points on the lower wing surface. The moments applied to the leading and trailing edges of the structural box by the portions of aerodynamic surfaces forward and rearward of the structural box are not considered, since they are small and tend to cancel out each other.

IV. Structural Weight Minimization

A. Design Model

For each configuration, a finite-element structural analysis model was created. Typically, the front wing semispan is divided into 12 bays spanwise and 5 panels chordwise. There are 12 ribs, plus front and rear spars. The optimization techniques to be described are applied to determine the thickness distribution of the cover skins, spars, and ribs to minimize the structural weight. The studies in Refs. 2 and 3 allowed all elements representing the cover skin to have different thicknesses so that detailed thickness distributions can be observed. In this study, the wing cover skins are

divided into regions, (see Fig. 6) and all elements belonging to the same region are required to have the same thickness. However, the thicknesses of upper and lower surface elements are not linked. The same concept is applied to spars and ribs. Consequently, the number of thicknesses that can be design variables are less than 64 throughout of this study, even though more than 400 finite elements are involved.

Design constraints are imposed on the von Mises combined stresses computed at the centroid of all the elements for all load cases. The thicknesses of the interwing joint structure are fixed and are not a part of the design variable set, but all element stresses of the joint are monitored and are kept within allowable bounds during the weight minimization phase.

Minimum gauge constraints are imposed on all panel thicknesses. The minimum thickness selected for the aluminum panels requires consideration of local buckling, lightning strikes, and manufacturing requirements. It has a significant impact on the structural weight of the wing. No explicit constraint on overall column buckling was applied, since this has already been studied for the configuration of Refs. 2 and 3, and has proven to be a nonlimiting condition with a sufficient margin. However, buckling analyses performed on optimal designs later revealed that the margins of buckling constraints were decreased when the joint locations were moved inboard.

B. Structural Weight Minimization Program

The structural weight minimization scheme is based on the PROSSS system[6] developed at NASA Langley Research Center. PROSSS implements the approximation concepts described in Ref. 8, using SPAR[9] as the finite-element structural analysis and database management module, and adopts CONMIN[10] as an optimizer. Reference 6 presents complete data, runstream procedures, and the front and end processors for the weight minimization of an aircraft fuselage section implemented on CDC 6600 at NASA Langley. For the present study, the PROSSS system was modified to accommodate the weight minimization for the joined-wing structures using EAL/EISI[11] in place of SPAR, and adding capabilities to handle fixed-size elements and stress-constraint screening. Approximately 30% of the code was modified, and it was implemented on the CRAY-XMP at NASA Ames Research Center.

Given a new configuration, it takes about 5 to 8 man-hours and 30 to 60 min of CPU time on a CRAY-XMP to complete a weight minimization. Since this is a strength design, the fully stressed design cycle is applied at the beginning to find an initial design for the complete optimization. The fully stressed design process usually provided good starting design even though the process was not carried out to its convergence.

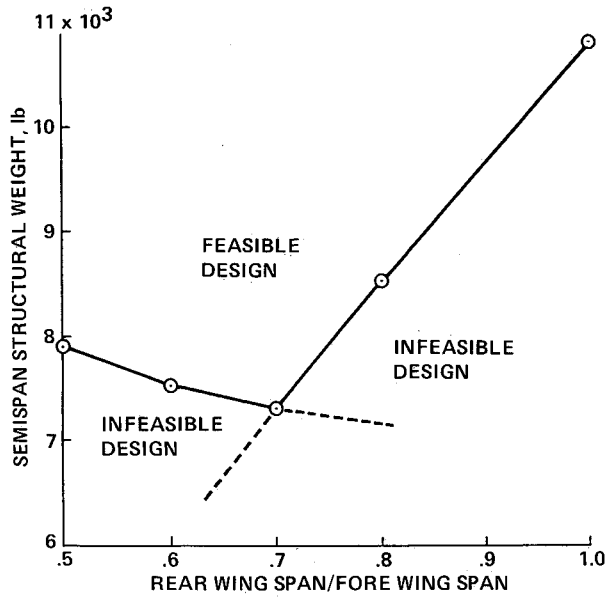

Fig. 7 Structural weight vs joint location.

C. Estimation of Wing Weight

The nonstructural weight of the wing may be of the same order as that of the structural weight. The nonstructural weights include leading- and trailing-edge boxes, control surfaces, actuator and actuator links, rivets, fuel tanks, and fuel. Since the control surfaces have not yet been designed, no attempts have been made to estimate the trailing-edge box and control surfaces; hence, the only nonstructural weight that may be reasonably estimated at this stage is that of the leading-edge skin. This part is assumed to be covered by aluminum panels of minimum gage. The rib weight in the leading-edge structural box is computed to be about 35% of the weight of the leading-edge skin. For most of the cases studied, the leading-edge weight turned out to be less than 1% of the weight of the structural box, and it is included in the structural weights listed in the table in the Appendix. The weight of the interwing joint is also included in the structural weight.

V. Numerical Results

Six examples of trend studies are presented in this section. Since these studies were performed at the request of airplane designers who were performing conceptual design, the design was varied from a fixed, specific reference design. Geometric parameters for the reference design are given below in Table 1, and deviations from this reference design are given with each specific study. A complete list of all the relevant configurations studied is summarized in the Appendix.

A. Joint Location Study

Based on the flatwise bending moment diagram given in Fig. 4, it was suggested that the joint position should be moved inboard to reduce M_x. Aerodynamically, the inboard joint configuration is not as desirable as the tip joint location because of the reduced span efficiency. It is thus necessary to have a quantitative evaluation of its weight advantage (if any) to perform trade-off studies of the complete system. Almost all geometric parameters are affected by the joint location, so a decision was made to modify the joint position such that the aspect ratio of the fore wing is kept equal to that of the rear wing. The geometric parameters that differ from the reference design are the fore wing dihedral angle (10.0 deg), and the rear wing dihedral angle (−30.0 deg). The span ratio (rear wingspan/fore wing span) was varied from 0.5 to 1.0. The area ratio was set equal to the square of the span ratio; thus, it varied from 0.25 to 1.0.

The structural weights of the wing for five joint locations are summarized in Fig. 7. Since the five data points given here are optimized minimum weights for the given configurations, the two separate branches (Fig. 7) may be considered to correspond to different sets of active constraints. The minimum weight designs for a wing with its joint location placed between 70 and 100% of the fore wing span have a different

Table 1 Geometry of baseline joined wing

Fore wingspan	100 ft
Total projected wing area	1,300 ft^2
Area ratio (rear wing/fore wing)	0.3
Fore wing sweep (quarter chord)	30.45 deg
Rear wing sweep (quarter chord)	−31.45 deg
Fore wing dihedral	5.0 deg
Rear wing dihedral	−22.4 deg
Fore wing taper ratio	0.4
Rear wing taper ratio	0.6

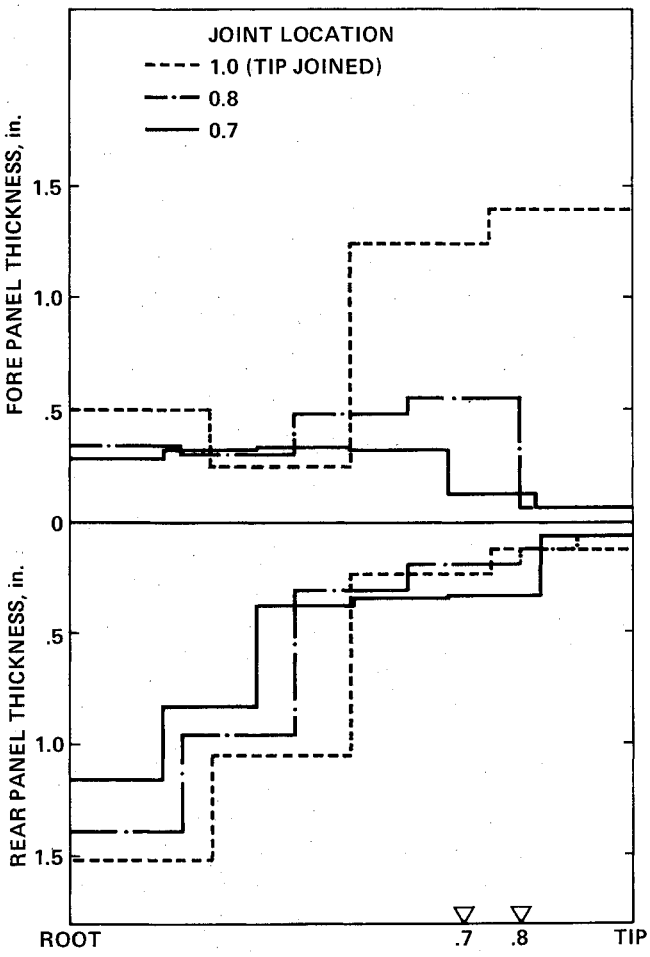

Fig. 8 Front wing, lower skin-thickness distribution vs joint location.

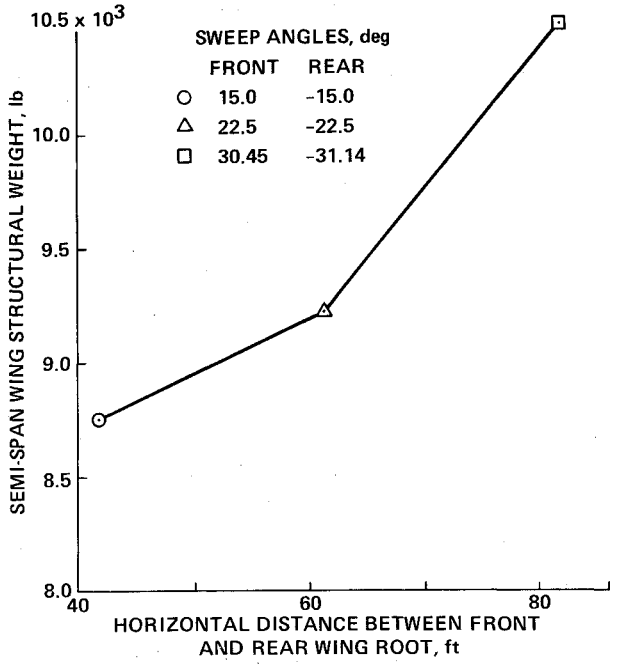

Fig. 9 Effect of sweep on joined-wing structural weight.

Table 2 Geometry variations for sweep study

Fore wing span, ft	120	120	120
Span ratio	0.6	0.6	0.6
Fore wing sweep angle, deg	15.0	22.5	30.45
Rear wing sweep angle, deg	−15.0	−22.5	−31.14
Horizontal distance between root quarter chords, deg	41.4	61.2	81.9

Table 3 Geometry variations for dihedral study

Fore wingspan, ft	120	120	120
Span ratio (rear/fore)	0.6	0.6	0.6
Fore wing dihedral angle, deg	5.0	7.5	10.0
Rear wing dihedral angle, deg	−22.4	−26.0	−30.0
Vertical separation of the fore and aft wing roots, ft	37.5	45.5	53.9

active stress constraint set compared to optimum wings with their joints between 50 and 70% of the fore wing span. The steep decrease in the structural weight due to the joint position shifting from tip to inboard positions may be attributed to two factors observed in Fig. 8, which illustrates lower skin thickness vs the spanwise ordinate (the upper skin thickness variation is similar). First, the wing-tip portion outboard of the joint is free from the end loads; thus, it is subjected to a very small bending moments, permitting the cover thicknesses to approach minimum gauge. Second, the root bending moment is decreased because of increased axial forces, resulting in a consistent thickness reduction for the inboard rear panels. On the other hand, if the joint position moves too far inboard (e.g., beyond 70%), then the part outboard of the joint, which behaves as a cantilever, lengthens and the weight penalty associated with the cantilever portion overwhelms the advantages of the joined portion. Note that this result does not necessarily imply that the optimal joint position is about 70% of the span of the fore wing. For example, if it is necessary to keep the height of the vertical stabilizer constant, it is also necessary to change sweep and dihedral angles, together with the joint position. For such cases, additional studies will be necessary.

B. Wing Sweep Angle

Perturbations of the sweep angles were carried out for geometry variations from the reference design as shown in Table 2.

The optimized wing structural weights are presented in Fig. 9. When the sweep angle increased while holding spans and dihedral angles constant, the plane that included the elastic axes of the two wings approached the x-y plane in Fig. 1; therefore, the lift force was distributed more to the out-of-plane components and the advantage of having bracing was reduced. Furthermore, the physical length of the wing increased and its structural boxes became more slender. All of these effects contributed to increase the wing structural weight as the sweep angles were increased.

C. Dihedral Angles

The dihedral angles were perturbed from the reference design as shown in Table 3.

Minimum weights corresponding to the three sets of dihedral angles are presented in Fig. 10. Increased dihedral angles make the bracing of the rear wing more effective; thus, the wing structural weight decreases.

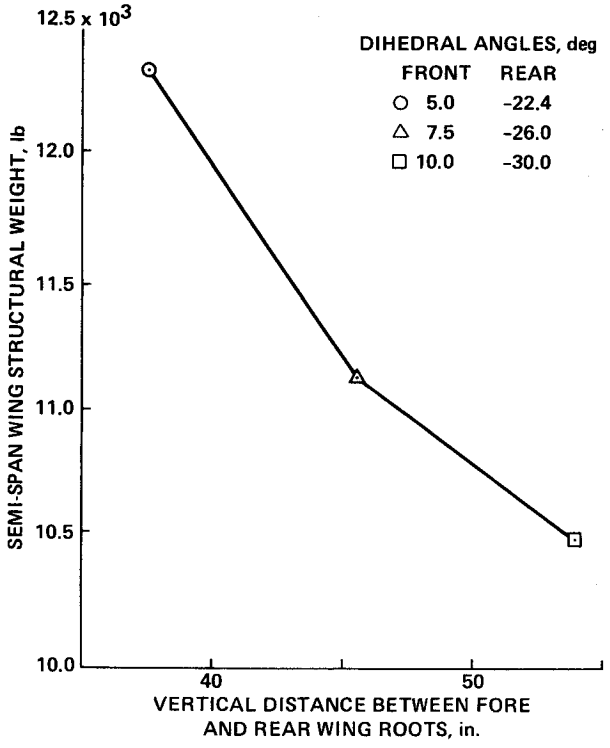

Fig. 10 Effect of dihedral on joined-wing structural weight.

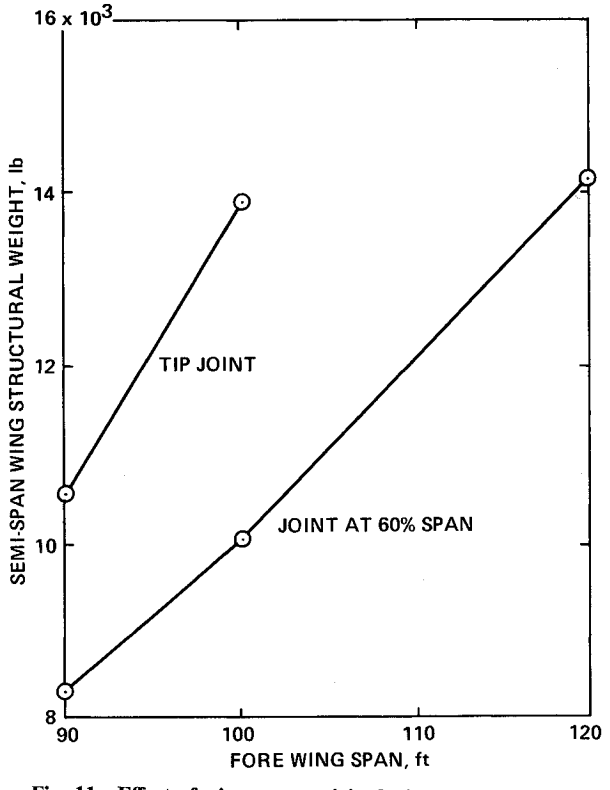

Fig. 11 Effect of wing span on joined-wing structural weight.

D. Wingspan

Effects of front wing span changes were studied for two joint locations corresponding to span ratios of 60 and 100% (tip-joined). For both cases, the wing span was perturbed to 90, 100, and 120 ft. The weight results are summarized in Fig. 11. This figure presents consistent trends with other results not reported in this paper.

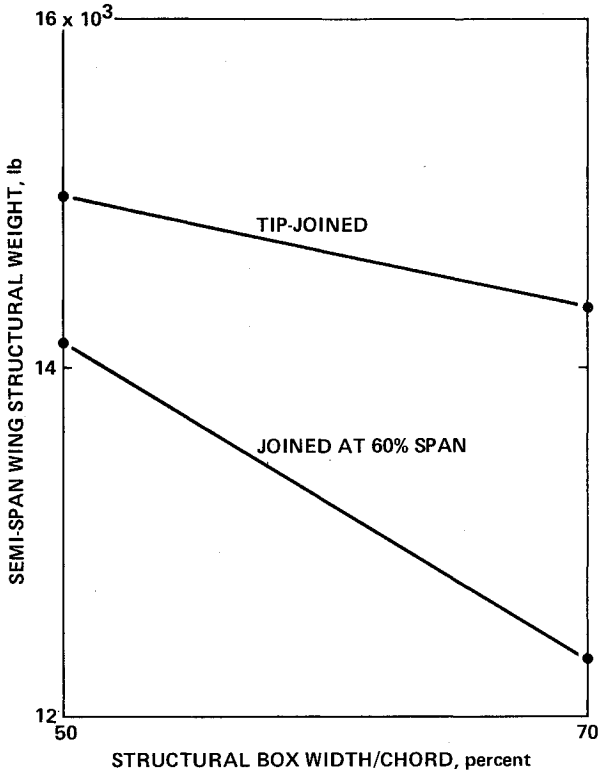

Fig. 12 Effect of structural box size on joined-wing structural weight.

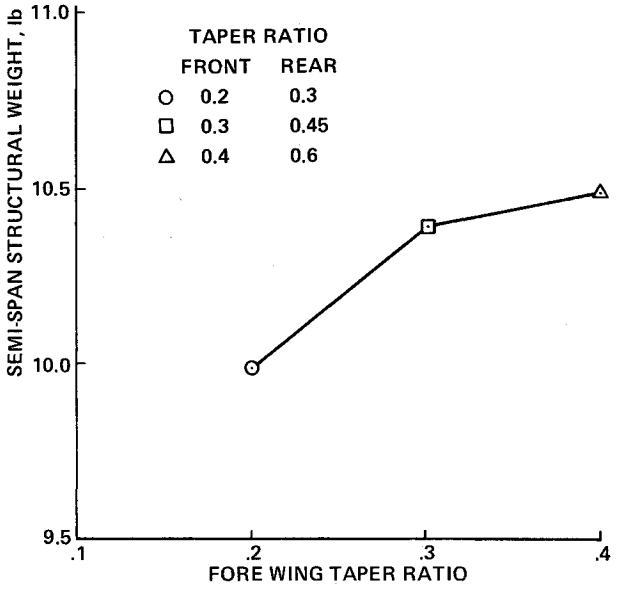

Fig. 13 Effect of structural box taper ratio on joined-wing structural weight.

E. Structural Box Width

As described in Sec. II, the material distribution over the inboard sections of both wings may follow the pattern shown in Fig. 3. Since a significant portion of the wing structural weight is in the inboard sections, weight reductions may be achieved by increasing the width of the structural box near the root because the effective depth in Fig. 3 is increased. Geometric parameters that differ from the reference design are the span ratio (0.6 and 1.0), and the fore wingspan (120 and 100 ft). For both joint locations, we considered structural box widths of 50% (15–65%) chord and 70% (5–75%) chord. The results, summarized in Fig. 12, indicate that weight is de-

Table 4 Geometry variations for taper study

Span ratio	0.6	0.6	0.6
Fore wingspan, ft	120	120	120
Fore wing dihedral, deg	10.0	10.0	10.0
Rear wing anhedral, deg	−30.0	−30.0	−30.0
Taper ratios			
Fore wing	0.2	0.30	0.4
Rear wing	0.3	0.45	0.6

creased by increasing the structural box width from 50 to 70% of the chord. A preliminary study showed that this trend is reversed for the cantilever configuration.

To exploit these characteristics, one should design the inboard structural box to be as wide as possible and use narrow structural boxes outboard of the joint. The width of the structural box within the given airfoil will depend on control-surface and associated auxiliary system design, and, thus, it cannot be considered as a structural design parameter. However, the results of this study indicate opportunities to save structural weight. For example, the structural box width may be made variable throughout the span, so that the structural box occupies 70% or more of the chord inboard, but reduces to 50% or less toward the tip. If the joint is not located at the tip, the portion outboard of the joint should use a narrow structural box, since this portion is a cantilever structure.

F. Taper Ratio

Wingtaper ratio is an important aerodynamic design parameter. However, the taper ratio of the structural box need not be identical to that of the aerodynamic surface. Hence, structural designers may have some freedom to modify this parameter even after the aerodynamic design is fixed. For our study of taper effects, the geometric parameters that were different from the reference design were as shown in Table 4. The spanwise loading distribution was kept constant for all taper ratios. The results obtained are shown in Fig. 13. Optimum weights were consistently decreased by increasing the taper. This trend can be predicted, because significant parts of the panels toward the tip of the wings are not fully stressed even for designs with low aspect ratios; hence, they can employ smaller structural boxes.

VI. Concluding Remarks

The structural weights of joined wings were evaluated for various configurations to provide weight trend data for aircraft conceptual design. The use of structural optimization was essential to obtain the weight trends. For example, the results describing the relation between structural weight and joint location could never have been obtained without carrying out structural optimization.

Over 50 cases of structural weight minimization were performed. The results indicated that structural weight characteristics depend strongly upon the wing geometry and structural arrangement, providing interesting opportunities to aircraft designers.

For structural analysis, a finite-element analysis program, EAL/EISI, was used. The analytic models were relatively simple, to reduce the data preparation and processing turnaround time. Also, the weights estimated in this study are limited to the structural-box and the leading-edge-section weights. Trailing-edge, control-surface, and auxiliary component weights were excluded. Thus, for more detailed analyses and for estimation of the total wing-weight evaluations, further studies will be required. These may include the modeling of fuselage and vertical stabilizer, and the addition of detailed models for spar caps and panel stiffeners for local panel stability. Studies of static and dynamic aeroelastic characteristics should also be performed. Furthermore, applications of advanced materials may provide additional parameters to be varied in the quest for the best design. The joined wing appears to offer promising opportunities for reducing structure weight, and deserves further study.

Appendix

This appendix summarizes some of the structural weight minimization results relevant to the studies reported in this paper. A standard design is selected for each joined wing and cantilever wing configurations, and weights for perturbed configurations are summarized in a tabular form. The wing structural weight for joined-wing configurations includes the weight of joint structures. The wing structural weight for cantilever wing configurations includes estimated horizontal-tail structural weight. The total lift is given per semispan but includes the front plus rear lifting surfaces in all cases. The lifting surface areas given are projected on the x-y plane.

Table A1 Lifting surface system structural weights: parametric study

Standard cases	Joined wing		Cantilever wing	
Front wingspan, b_F, ft	120.00		120.00	
Span ratio, B, b_R/b_F	0.60		0.40	
Front wing area, S_F, ft^2	1,000.00		1,000.00	
Area ratio, S_R/S_F	0.30		0.30	
Total lift, L, lb	318,750.00		318,750.00	
Semispan wing Structural weight, lb	10,490.00		16,638.00	
	Front	Rear	Wing	Tail
Taper ratio	0.40	0.60	0.30	0.30
Dihedral angle, deg	10.00	−30.00	3.00	0.00
Sweep angle, deg	30.45	−31.14	30.00	30.00
Airfoil thickness, t/c	0.12	0.12	0.12	0.12
Minimum skin gage, in.	0.06	0.06	0.06	0.06
Structural box/chord	0.70	0.70	0.50	0.50

Table A2 Lifting surface system structural weights: effects of variations

Joined wing cases

Case ID	Span ft	Span ratio	F. wing area ft^2	Area ratio	Sweep angles F/R, deg	Dihedral ratios F/R, deg	Taper ratios F/R	Str. box width/Chord lb	Total lift lb	Str. weight semispan lb
Standard case										10,490
1	90.0					5.0/−22.4		0.5		8,327
2	100.0					5.0/−22.4		0.5		10,018
3						5.0/−22.4		0.5		14,141
4						5.0/−22.4				12,334
5						7.5/−26.0				11,192
6	100.0		800.0			7.5/−26.0		0.5		12,159
7	90.0	1.0	650.0			5.0/−22.4		0.5		10,537
8	100.0	1.0				5.0/−22.4		0.5		13,852
9		1.0	650.0			5.0/−22.4		0.5		20,378
10	100.0	1.0	1,040.0			5.0/−22.4		0.5		9,978
11	100.0	1.0	520.0			5.0/−22.4		0.5		14,984
12	100.0	1.0	520.0			5.0/−22.4		0.5		14,349
13									159,375	5,334
14	100.0		520.0						159,375	7,303
15		0.5								11,710
16					22.5/−22.5					9,207
17					15.0/−15.0					8,752
18							0.2/0.30			9,986
19							0.3/0.45			10,398
20	100.0	0.5	1,040.0	0.25						7,895
21	100.0		956.0	0.36						7,542
22	100.0		872.0	0.49						7,307
23	100.0		793.0	0.64						8,524
24	100.0	1.0	650.0	1.00						10,825
25	90.0	0.7	872.0	0.49						6,016
26		0.7	872.0	0.49						10,809

Cantilever wing cases

Case ID	Span ft	Span ratio	F. wing area ft^2	Area ratio	Sweep angles deg	Dihedral ratios deg	Taper ratios F/R	Str. box width/Chord lb	Total lift lb	Str. weight semispan lb
Standard case										16,638
1	90.0									7,738
2	100.0									10,197
3								0.7		18,987
4	100.0		800.0							12,221
5	100.0							0.7		13,736
6									159,375	8,570
7					22.5/−22.5					15,377
8					15.0/−15.0					15,048
9							0.5/0.5			18,137

Acknowledgments

The authors wish to express their appreciation to Dr. I. Kroo of NASA Ames Research Center (currently at Stanford University) for valuable discussions and for providing a computer program to compute the aerodynamic lift distribution. Mr. T. Gregory of NASA Ames Research Center stimulated initiation of this study and provided continuous support. The authors would like to thank Dr. J. Sobieski and Mr. J. Rogers of NASA Langley Research Center for providing the PROSSS system.

References

[1]Wolkovitch, J., "The Joined Wing: An Overview," *Journal of Aircraft*, Vol. 23, March 1986, pp. 161–178.

[2]Fairchild, M. P., "Structural Weight Comparison of a Joined Wing and a Conventional Wing," M.S. Thesis, Univ. of Texas, Arlington, TX, May 1980.

[3]Samuels, M. F., "Structural Weight Comparison of a Joined Wing and Conventional Wing," *Journal of Aircraft*, Vol. 19, June 1982, pp. 485–491.

[4]Hajela, P., "Weight Evaluation of the Joined Wing Configuration," NASA CR-166592, June 1984.

[5]Wolkovitch, J. and Lund, D. W. "Application of the Joined Wing to Turboprop Transport Aircraft," to be published as a NASA Contractor Rept. on Contract Number NAS2-11255.

[6]Rogers, J. L., Sobieski, J., and Bhat, R. B., "An Implementation of the Programming Structural Synthesis System (PROSSS)," NASA TM-83180, Dec. 1981.

[7]Kroo, I., "Tail Sizing for Fuel Efficient Transports," AIAA Paper 83-2476, Oct. 1983.

[8]Schmit, L. A. and Miura, H., "Approximation Concepts for Efficient Structural Synthesis," NASA CR-2552, March 1976.

[9]Whetstone, W. D., "SPAR: Structural Analysis System Reference Manual," NASA CR-158970-1, 1978.

[10]Vanderplaats, G. N., "CONMIN—A Fortran Program for Constrained Function Minimization—User's Manual," NASA TM-X-62,282, Aug. 1973.

[11]Whetstone, W. D., "EISI-EAL Engineering Analysis Language Reference Manual," Engineering Information Systems, Inc., San Jose, CA, July 1983.